Optical Materials 42 (2015) 204–209

Contents lists available at ScienceDirect

Optical Materials

journal homepage: www.elsevier.com/locate/optmat

# Concentration quenching, surface and spectral analyses of $SrF_2:Pr^{3+}$ prepared by different synthesis techniques

M.Y.A. Yagoub, H.C. Swart, E. Coetsee *

*Department of Physics, University of the Free State, PO Box 339, Bloemfontein ZA9300, South Africa*

ARTICLE INFO

*Article history:*
Received 4 September 2014
Received in revised form 10 January 2015
Accepted 12 January 2015
Available online 7 February 2015

*Keywords:*
$SrF_2:Pr^{3+}$
Concentration quenching
XPS
PL

ABSTRACT

$Pr^{3+}$ doped strontium fluoride ($SrF_2$) was prepared by hydrothermal and combustion methods. The phosphors were characterized by X-ray diffraction (XRD), scanning electron microscope (SEM), X-ray photoelectron spectroscopy (XPS) and Photoluminescence (PL) spectroscopy. XRD patterns indicated that the samples were completely crystallized with a pure face-centred cubic (space group: Fm3m) structure. SEM images showed different morphologies which is an indication that the morphology of the $SrF_2:Pr^{3+}$ phosphor strongly depends on the synthesis procedure. Both the $SrF_2:Pr^{3+}$ samples exhibit blue–red emission centred at 488 nm under a 439 nm excitation wavelength ($\lambda_{exc}$) at room temperature. The emission intensity of $Pr^{3+}$ was also found to be dependent on the synthesis procedure. The blue–red emission has decreased with an increase in the $Pr^{3+}$ concentration. The optimum $Pr^{3+}$ doping level for maximum emission intensity was 0.4 and 0.2 mol% for the hydrothermal and combustion samples, respectively. The reduction in the intensity for higher concentrations was found to be due to dipole–dipole interaction induced concentration quenching effects.



## 1. Introduction

$Pr^{3+}$ is an interesting ion because it has multiple transitions that allows for detailed studies of both radiative and non-radiative mechanisms. $Pr^{3+}$ doped materials have been extensively investigated due to its potential use in a variety of applications [1–5]. For phosphor applications, the 4f–4f transitions are the most relevant, especially the $^1D_2 \rightarrow {}^3H_4$ red emission from $Pr^{3+}$ doped oxide materials [6,7]. Recently, the $Pr^{3+}$ ion was found to be a promising co-doped ion in the lanthanide-based luminescent materials to be used for quantum cutting with the Yb ion, which can be used to enhance the solar cell efficiency [1,8]. Quantum cutting with $Pr^{3+}$ requires a host material with a lower vibrational energy. Strontium fluoride ($SrF_2$) has very small cut-off phonon energy (~350 $cm^{-1}$) and was found to be a good host for the quantum cutting application [1,8].

The $SrF_2:Pr^{3+}$ system has been investigated by several researchers [5,9,10] and the majority reported the photon emission cascade and energy transfer mechanism in $SrF_2$ doped with $Pr^{3+}$ ions (with the main focus on the $4f^n$–$4f^{n-1}5d$ emission). The 4f–4f transitions have also been studied, but most of these results have been devoted to the red emission from $Pr^{3+}$ doped oxide materials [6,7,11]. On the other hand, it has been shown that the probability of the multi-phonon relaxation between $^3P_0$ and $^1D_2$ levels of $Pr^{3+}$ significantly decreases as the phonon energy of the host decreased [12]. It has also been observed that the emission intensity of the $^3P_0$ state of the $Pr^{3+}$ doped host with a small phonon energy decreased with increasing the $Pr^{3+}$ concentration. This was attributed to cross-relaxation processes [12–15]. This behavior normally occurs at the smaller average interionic distances between the $Pr^{3+}$ ions.

Most investigations on the concentration quenching of $Pr^{3+}$ doped crystals have been studied in oxide hosts. The different pathways by which cross-relaxation can take place makes $Pr^{3+}$ a challenging ion to study. The low phonon energy of the $SrF_2$ host may play a key role on the optical properties of the dopant ion. Furthermore, the emission intensities of lanthanide ions in a host were found to be strongly dependent on the condition of the synthesis procedure [8]. This was observed on $Pr^{3+}$ co-doped $Yb^{3+}$ in $SrF_2$ where the concentration quenching of both ions at small concentrations reduced the near infrared emission intensity and prevented more quantitative assessment of the quantum cutting efficiency. The $SrF_2$:Pr, Yb quantum cutting samples were synthesised by solid state reaction [8]. It is therefore quite meaningful to study the effect of different synthesis techniques on the concentration quenching of $Pr^{3+}$ in $SrF_2$ phosphor. In this paper, the surface and spectral investigation of $Pr^{3+}$ doped $SrF_2$ phosphor powders prepared by using both the hydrothermal and combustion methods

* Corresponding author.
*E-mail address:* Coetseee@ufs.ac.za (E. Coetsee).

http://dx.doi.org/10.1016/j.optmat.2015.01.011
0925-3467/

are studied. The concentration quenching of $Pr^{3+}$ for both methods was investigated.

## 2. Experimental

Cubic $SrF_2$ nanocrystals doped with $Pr^{3+}$ were prepared using hydrothermal and combustion synthesis procedures, as previously described [16,17]. For the hydrothermal synthesis, analytical grade of $Sr(NO_3)_2$, $Pr(NO_3)_3{\cdot}6H_2O$, $NH_4F$, sodium oleate, oleic acid and ethanol were used without further purification. For a typical synthesis of $SrF_2$:$Pr^{3+}$, ethanol, sodium oleate and oleic acid were added simultaneously to an aqueous solution containing $Sr(NO_3)_2$, $NH_4F$ and $Pr(NO_3)_3{\cdot}6H_2O$. After 10 min of stirring the milky colloidal solution was transferred to a 125 ml autoclave lined with Teflon and heated at 180 °C for 24 h. The product was collected by centrifugal and washed with water and ethanol. Finally, the product was dried for 24 h in an oven at 80 °C. The as-prepared $SrF_2$:$Pr^{3+}$ samples did not emit, therefore, they were sintered for 2 h at 450 °C.

In the combustion synthesis, an aqueous solution of $NH_4F$ was added drop wise to a mixture of $Sr(NO_3)_2$, $Pr(NO_3)_3{\cdot}6H_2O$ and urea, which was used as fuel. The milky solution was collected after thoroughly stirring. Then, the obtained solution was transferred into a porcelain crucible and placed in a furnace at 500 °C until the ignition occurred. Finally, the as-prepared powder was sintered for 2 h at 700 °C.

The phosphors were characterized by X-ray diffraction (XRD) (Bruker Advance D8 diffractometer with Cu Kα radiation ($\lambda$ = 0.154 nm)) to identify the crystalline structure of the powder. Photoluminescence (PL) and photoluminescence excitation (PLE) spectra were collected using a Cary Eclipse fluorescence spectrophotometer and Horiba scientific (Fluorolog-3) spectrofluorometer equipped with a xenon lamp. The surface morphology was recorded using a Shimadzu Supers-can scanning electron microscope (SEM) model ZU SSX-550. High resolution X-ray photoelectron spectroscopy (XPS) was obtained with a PHI 5000 Versaprobe system. A low energy $Ar^+$ ion gun and low energy neutralizer electron gun were used to minimize charging on the surface. A 100 μm diameter monochromatic Al Kα X-ray beam ($h\nu$ = 1486.6 eV) generated by a 25 W, 15 kV electron beam was used to analyze the different binding energy peaks. The pass energy was set to 11 eV giving an analyzer resolution ⩽0.5 eV. Multipack version 8.2 software was utilized to analyze the spectra to identify the chemical compounds and their electronic states using Gaussian–Lorentz fits. All measurements were performed at room temperature.

## 3. Results and discussion

Fig. 1(a) depicts the XRD patterns of $SrF_2$:$Pr^{3+}$ prepared by the hydrothermal and combustion method as well as the standard data for $SrF_2$ (card No. 00-086-2418). The strong diffraction peaks indicate that the samples powder is fully crystallized (face-centred cubic with space group: Fm3m). The patterns for doped samples with $Pr^{3+}$ are similar to those from the pure $SrF_2$ matrix. This indicates that there is no obvious influence of the dopants on the crystalline structure of the host. It can, however, be noticed that doping of $Pr^{3+}$ in both methods causes a slight shift to a higher angle with comparison to the standard data (Fig. 1(a)). This can be attributed to the radius difference between $Pr^{3+}$ (0.099 nm) and $Sr^{2+}$ (0.126 nm) ions, which confirms that $Pr^{3+}$ ions are incorporated into the $SrF_2$ lattice. The sintering temperature of the as-prepared hydrothermal samples caused a slight variation in the XRD intensities. The reason might be that, the orientation growth of the particles occurred in certain directions. The calculated $SrF_2$ lattice parameter is (5.778 ± 0.0025) Å and

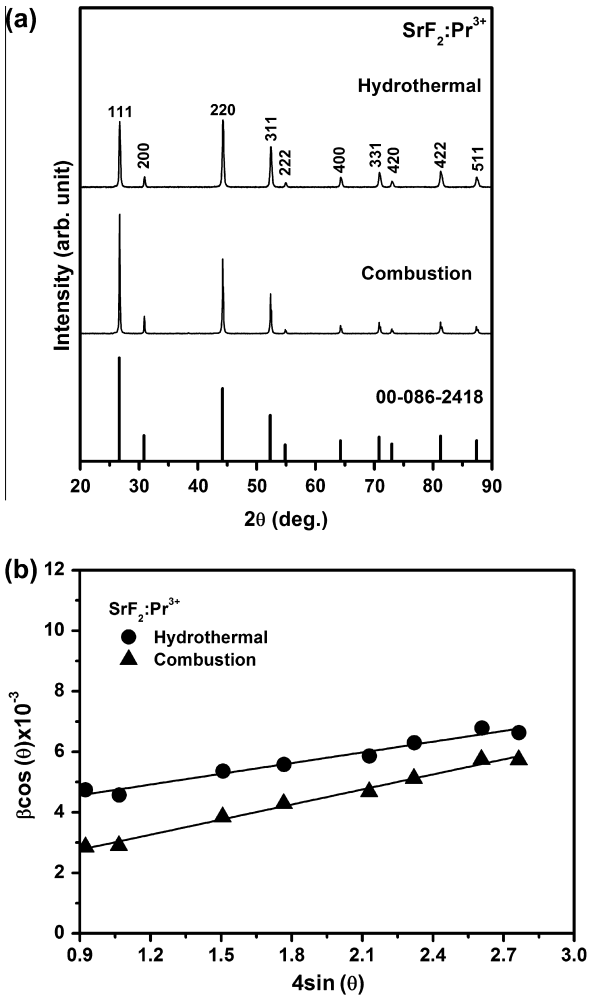


**Fig. 1.** (a) XRD patterns of $SrF_2$:$Pr^{3+}$ phosphors; (b) Williamson–Hall plots for $Pr^{3+}$ doped $SrF_2$ samples for both the hydrothermal and combustion methods.

(5.775 ± 0.0054) Å for the samples prepared by the combustion and hydrothermal methods, respectively. These results agreed well with reported values [17].

Fig. 1(b) shows Williamson–Hall plots for the combustion and hydrothermal samples, where the peak broadening is dependent on both crystallite size and microstrain. The Williamson–Hall equation is given by $\beta\cos\theta = K\lambda/\mathbf{S} + 4\varepsilon\sin\theta$, where $\lambda$ is the wavelength of the X-rays (0.154 nm) and $\beta$ is the full-width at half maximum of the X-ray peak at the Bragg angle $\theta$, $K$ is a shape factor taken as 0.9, **S** is the crystallite size and $\varepsilon$ is the microstrain [18]. The slope of this equation is equal to the microstrain and the crystallite size can be calculated from the intercept ($K\lambda/\mathbf{S}$). The microstrain of both the hydrothermal and combustion samples has values approximately of 0.0012 (0.12%) and 0.0017 (0.17%), respectively, showing only very small amount of microstrain in this produced materials. The bigger strain was produced by combustion synthesis, which might be true as the combustion technique requires a higher temperature. The estimated average crystallite size (**S**) of the particles was calculated from both the slope of the William–Hall equation and from the well-known Debye–Scherrer's equation [19]. These are tabulated in Table 1. This shows that the hydrothermal method produces a smaller particle size.

SEM images were obtained in order to investigate the surface morphology of the synthesized phosphors. Fig. 2 represents the SEM images that were taken from the powders that were prepared by the different synthesis methods ((a) combustion and (b)